

Making 5G Adaptive Antennas Work for Very Fast Moving Vehicles

Dinh-Thuy Phan-Huy

Orange, France

E-mail: dinhthuy.phanhuy@orange.com

Mikael Sternad

Uppsala University, Sweden

E-mail: Mikael.Sternad@signal.uu.se

Tommy Svensson

Chalmers University of Technology, Sweden

E-mail: tommy.svensson@chalmers.se

Abstract—Wireless systems increasingly rely on the accurate knowledge at the transmitter side of the transmitter-to-receiver propagation channel, to optimize the transmission adaptively. Some candidate techniques for 5th generation networks need the channel knowledge for tens of antennas to perform adaptive beamforming from the base station towards the mobile terminal. These techniques reduce the radiated power and the energy consumption of the base station. Unfortunately, they fail to deliver the targeted quality of service to fast moving terminals such as connected vehicles. Indeed, due to the movement of the vehicle during the delay between channel estimation and data transmission, the

channel estimate is outdated. In this paper, we propose three new schemes that exploit the “Predictor Antenna” concept. This recent concept is based on the observation that the position occupied by one antenna at the front of the vehicle, will later on be occupied by another antenna at the back. Estimating the channel of the “front” antenna can therefore later help beamforming towards the “back” antenna. Simulations show that our proposed schemes make adaptive beamforming work for vehicles moving at speeds up to 300 km/h.



IMAGE LICENSED
BY INGRAM PUBLISHING

I. Introduction

During the last decades, a major part of the data traffic demand in wireless communications has come from static and pedestrian users. As a consequence, cellular networks of the 2nd (2G) to 4th Generation (4G) are optimized to support high loads of static users with spectrum and power constraints. However, they are not designed to support large loads of vehicular communications.

This work has been performed in the framework of the FP7 project ICT-517669 METIS, which is partly funded by the EU. This paper is an extended version of the conference paper [27].

Digital Object Identifier 10.1109/MITS.2015.2408151
Date of publication: 20 April 2015

Thanks to the CSIT, the BS adapts its transmission to the current radio conditions and increases its efficiency in terms of spectrum usage and/or power consumption.

Indeed, many advances in signal processing for wireless systems exploit a powerful concept which is only useful for slow-moving users: “channel state information at the transmitter” (CSIT). The main idea is that the transmitter, for instance the base station (BS), is informed of the current radio conditions between itself and the receiver (for instance the terminal device). Thanks to the CSIT, the BS adapts its transmission to the current radio conditions and increases its efficiency in terms of spectrum usage and/or power consumption. Unfortunately, the CSIT of a fast moving user will be outdated and useless, due to the delay between the time when the channel is measured and the time when it is available at the transmitter. For fast moving users, 2G to 4G networks therefore fall back on CSIT-free techniques. These ensure that the target quality is met by spending more resources (in terms of bandwidth and/or power) than for a static user.

We expect that by the time the 5th generation (5G) is deployed, the gap in traffic demand between vehicular and static users will have rapidly decreased. It is thus time to investigate methods that enable CSIT usage, even for vehicular users.

A. 5G Adaptive Downlink Beamforming Is Not Robust to Speed

In time division duplex (TDD) wireless communications, channel reciprocity and CSIT can be exploited by multiple input single output (MISO) techniques, such as maximum ratio transmission (MRT) beamforming [1]. Such techniques can achieve a high performance, still with a low complexity [2]. Recent work has shown that very large antenna arrays at the BS have the potential to save energy

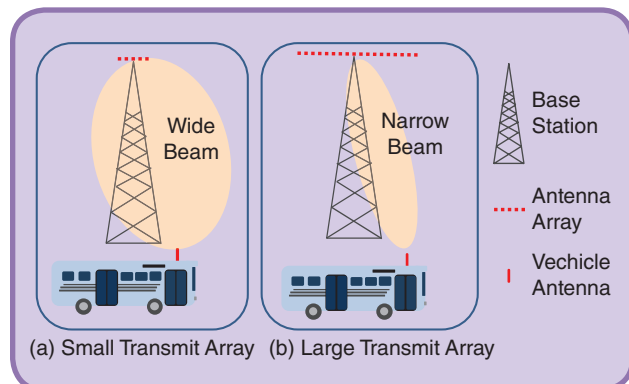


FIG 1 Adaptive downlink beamforming towards a vehicle, line-of-sight propagation scenario.

without performance degradation [2–5]. The theoretical transmit energy saving at the BS increases linearly with the number of uncorrelated transmit antennas [3–5], if the beamforming can be performed accurately. These “massive antenna configurations” are currently being studied for the future

5th Generation (5G) networks [6].

In a conventional TDD transmit beamforming system, which we will refer to as “Reference System” (RS), the mobile station sends known pilot symbols in the uplink. The BS acquires channel state information at the transmitter to predict the channel, and then computes beamforming weights. Shortly thereafter, the BS transmits data in the downlink using these weights. Thanks to the beamforming, a target signal-to-noise ratio (SNR) can be attained at a lower transmit power, as compared to the single-antenna case: *the BS saves transmit energy*. Alternatively, we may use the beamforming to increase the transmission range, reduce coverage holes and increase the data rate, without increasing the transmit power.

Due to the time delay between channel estimation and downlink transmission, the channel estimate is always outdated for a moving terminal. If this time delay is short, it is no major problem in an ideal free space line-of-sight propagation environment. An antenna array then simply forms a beam, as illustrated by Fig. 1. This beam is typically much wider than the distance the vehicle travels from the time the channel is estimated to the time when the downlink transmission takes place. The transmit beam is then slightly misplaced due to the time delay, but the receiver antenna on the vehicle is still positioned well within the beam. In this case, the mispointing of the beam does not impact the performance of the system.

The situation is very different in the common case of a multipath fading environment, where non line-of-sight propagation is significant. In this case, the result of the adaptive transmit beamforming can no longer be described as a simple beam.

Let us first consider the particular case where a single antenna at the BS is applying a maximum ratio transmission beamforming weight to its transmission. The net effect of reflections of scattering from multiple objects in the environment on the energy transmitted by the antenna can then be described by a standing wave pattern in the vicinity of the receiver antenna. This pattern has peaks (power maxima) separated by around half a carrier wavelength, as illustrated by Fig. 2a. These peaks constitute a main beam at the target receive antenna surrounded by side beams. In this Single Input Single Output (SISO) configuration, the main beam and the side beams have comparable strengths, and no beamforming gain is observed.

In the MISO case, the phenomenon described for the SISO case in a multi-path environment will occur for the transmissions from all transmit antennas in an antenna array, as illustrated by Fig. 2b. The maximum ratio transmission beamforming is designed to adjust the phases of the signals from all transmit antennas so that the phases add constructively at the precise location of the receiver antenna. This does not result in a clean and regular narrow beam in the area of the target receiver. Instead, the system creates a strong main beam centered on the receiver antenna, surrounded by weak side beams spaced by half a wavelength on average. As a consequence, if the vehicle moves by only a fraction of a carrier wavelength between the time the channel is estimated and the instant when transmission takes place, the receive antenna is off the center of the main beam. Beamforming mispointing now becomes a problem. Indeed, the signal to noise ratio and the Block Error Rate (BLER) targets are then not attained. Also, the effect of mispointing is more severe when the BS antenna array is larger, as confirmed by studies conducted in [7], [8].

B. The Predictor Antenna Concept

Extrapolating previous channel samples using Wiener or Kalman prediction can improve the situation in some scenarios [9–13]. However, these techniques cannot reliably predict multipath fading channels by more than approximately 0.2–0.3 carrier wavelengths in space. This has been verified by extensive measurement-based evaluations in [10], [11], and [13]. Such prediction horizons are inadequate at vehicular velocities for carrier frequencies above 1 GHz [14].

The key challenge that motivates our present work is to develop enablers for the use of precise channel state information at the transmitter also in situations with multipath fading channels rapidly varying in space. This would enable the use of the most advanced transmission models and techniques in our arsenal also for high data rate radio transmission to vehicles.

Recently, motivated by the problem of designing high-performance links to vehicular moving relays, the works [14–15] have introduced the new fundamental concept of “Predictor Antenna”. A predictor antenna is positioned on the roof of a vehicle and one or several separate receive antennas are aligned behind the predictor antenna. The vehicle is assumed to move through a stationary electromagnetic standing wave pattern. In other words, the BS creates a time-invariant pattern, and the vehicle simply moves through it. Due to this movement, receive antennas naturally replace the predictor antenna and see the same channel as the predictor antenna, but simply a bit later. Known pilot signals transmitted to the base station from the predictor antenna can therefore be used to predict the channel of the receive antennas. This generic concept is an enabler for any technique based on channel state information at the transmitter. It is not restricted to TDD and it is applicable

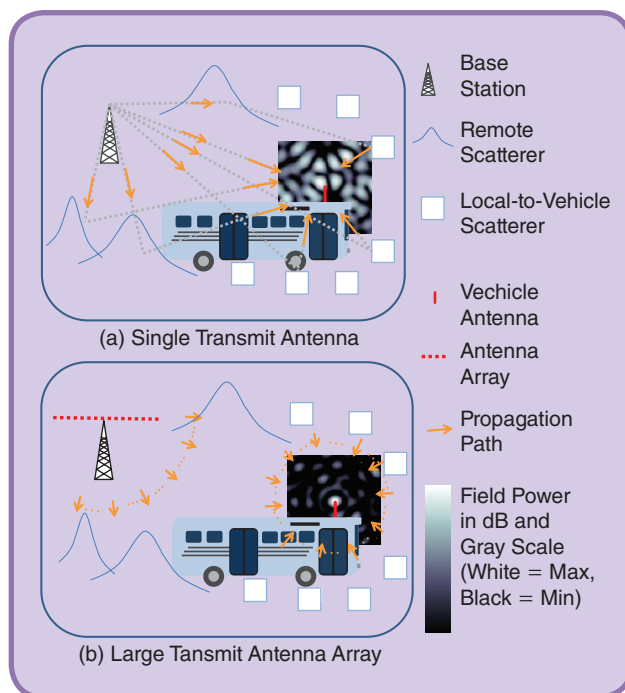


FIG 2 Adaptive downlink beamforming towards a vehicle, non line-of-sight propagation scenario.

to downlink and uplink. Further analysis and experimental validation of the concept with a vehicle in outdoor urban areas has been conducted in [14], [16–20].

Recently, for the particular purpose of large MISO downlink beamforming in TDD, a closely related scheme called Separate Receive and Training Antennas (SRTA) [8], has furthermore been proposed to achieve high energy efficient wireless downlinks towards very fast moving vehicles. The vehicle roof has one predictor antenna at the front and several “Candidate Antennas” aligned behind. The predictor antenna sends pilots in the uplink and the BS computes beamforming weights. Among the candidate antennas, a “Receive Antenna”, responsible for data demodulation, is dynamically selected among the candidate antennas as a function of the vehicle speed. The TDD frame is also dynamically extended. The receive antenna is selected and the extended frame is computed to ensure that, during the downlink phase, the receive antenna is at the position that was previously occupied by the predictor antenna during the uplink phase. A somewhat similar scheme was proposed in [21]. There, antennas on the vehicle roof were transmitting successively to perform uplink beamforming from a roughly fixed position in space.

C. Contribution

Current standards support frame extensions with a time granularity of 1 ms [22]. However, with such a coarse granularity, SRTA performance still suffers from residual beamforming mispointing [8].

We here propose and investigate three schemes based on the SRTA scheme, with the aim to improve its robustness when it is used for large MISO downlink beamforming in TDD.

We first investigate two low complexity approaches which consist in muting some transmit antennas to widen the beam when mispointing is too severe. Two schemes are studied, denoted the “border Switch Off Scheme” (BSOS) and the “Random Switch Off Scheme” (RSOS).

We then explore a more complex approach, using a “Polynomial Interpolation” scheme. In this scheme, all antennas at the vehicle may be used as a Predictor Antenna Array, and all of them may send uplink pilot symbols. Uplink measurements are collected from the transmission from all antennas during multiple periods, to obtain channel estimates over a dense pattern of positions in space. As these positions surround the position for which the channel must be predicted, interpolation can provide an accurate estimate of the desired channel component. This strategy will be illustrated here by using polynomial interpolation.

The paper is organized as follows. Section II presents our generic transmission model. Scheme-specific parameters are detailed in section III. Section IV gives an initial analysis which is then validated and complemented by simulation results presented in section V. Section VI concludes the paper.

The following notations are used throughout the paper: $\vec{v} \in \mathbb{R}^3$ is a vector with Cartesian coordinates; if $u \in \mathbb{R}$, $[u]$ is the integer part of u ; if $u \in \mathbb{C}$, $|u|$ is its module; if $\vec{v} \in \mathbb{R}^3$, $\|\vec{v}\|$ is its norm and $[a, b[= x \in \mathbb{R} \mid a \leq x < b$.

II. Common System Model

This section presents common parameters and constraints for the proposed and investigated downlink transmit schemes.

We consider a downlink wireless backhaul link between a BS and a vehicle moving with a velocity vector \vec{v} and speed $v = \|\vec{v}\|$. All investigated schemes use MISO maximum ratio transmission beamforming weights based on channel state information at the transmitter, and they all target the same signal to noise ratio x_T . The required prediction horizon between the acquisition of the channel state information at the transmitter and the data transmission is at least t_0 , with t_0 being the minimum time required for processing at the BS.

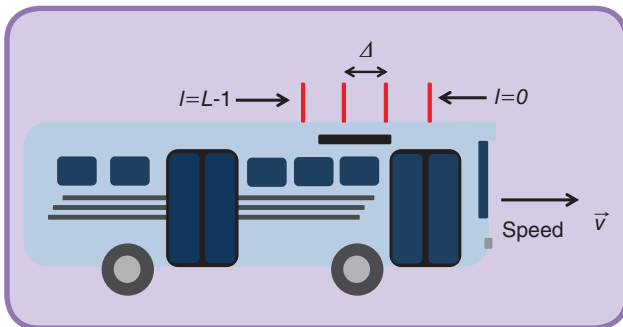


FIG 3 Vehicle antennas.

A. Antennas and Positions at Different Times

The BS has K transmit antenna(s), each with an index $k \in A_0$, with $A_0 = \{k \in \mathbb{N}, 0 \leq k < K\}$. A subset $A \subseteq A_0$ of K_a antenna(s) is active.

The vehicle has L antenna(s), each with an index $l \in \Lambda$, with $\Lambda = \{l \in \mathbb{N}, 0 \leq l < L\}$. Among these antennas, for simplicity of exposition, one antenna called the “receive antenna” is of interest in the downlink. It is to receive a beamformed downlink transmission that is then demodulated and decoded. Furthermore, a set of P antenna(s) $\Pi = \{l \in \mathbb{N}, 0 \leq l < P\}$ included in Λ , called “predictor antenna(s)”, is responsible for sending pilots in the uplink. We use l_a to denote the index of the receive antenna.

Let \vec{n}_l^m and $\vec{n}_l^{t'}$ be the position vectors of the antenna number l at the specific times τ^m and t' (to be defined later on), respectively. As illustrated by Fig. 3, the antennas of the vehicle are placed on the roof and are all spaced by an equal distance Δ . The antenna positions are aligned with the vehicle direction of travel \vec{v} behind the front antenna (i.e. the antenna with index $l = 0$). The position vectors \vec{n}_l^m and $\vec{n}_l^{t'}$ therefore satisfy the following conditions:

$$\vec{n}_l^t - \vec{n}_0^t = \vec{n}_l^m - \vec{n}_0^m = -l\Delta v^{-1}\vec{v}, \quad (1)$$

$$\vec{n}_l^{t'} - \vec{n}_l^m = (t' - \tau^m)\vec{v}. \quad (2)$$

We define $\vec{\alpha}$ as the position of the front antenna of the vehicle at time τ^0 . With this notation, we can thus write:

$$\vec{\alpha} = \vec{n}_0^0. \quad (3)$$

We define $\vec{\varepsilon}$ as the position of the receive antenna (i.e. the antenna with index $l = l_a$) at time t' . With this notation, we can thus write:

$$\vec{\varepsilon} = \vec{n}_{l_a}^{t'}. \quad (4)$$

B. Static Spatially Correlated Channel Model

The vehicle is assumed to be moving in a time-invariant and spatially correlated fading propagation channel, which will be further described in section V-A. This assumption has been verified experimentally in [16–20]. Measurement-based investigations [19] have shown that a very high correlation can be obtained between the propagation channels from/to two antennas on a vehicle that at different time instants move through the same position. In this paper, we assume that the two channels seen by two antennas successively occupying the same position in space are exactly equal.

Orthogonal Frequency Division Duplex (OFDM) is assumed. Hence, for a given sub-carrier and OFDM symbol, the channel gain between BS antenna k and any antenna at position \vec{n} can be modeled by a complex coefficient $g_k(\vec{n})$.

C. Channel Prediction and Beamforming

We consider a TDD frame, with uplink and downlink periods $[-\tau^{UL}, 0[$ and $[0, \tau^{DL}]$, respectively.

Both the acquisition of the channel state information at the transmitter and the beamforming operation are performed on a per OFDM symbol and per sub-carrier basis. For each transmitted downlink data symbol, sub-carrier and antenna, the BS computes a beamforming weight based on one or several channel coefficient measurement(s). Therefore, the BS uses two distinct beamformers for two consecutive symbols of the same frame.

Such a tight adaptation of the transmission to the current channel condition is useful for extremely high speeds or extremely large frames. However, it is unnecessarily complex for lower speeds. In practice, the frequency for the update of beamforming coefficients in the time domain and frequency domain would be optimized according to the channel coherence time and the channel coherence bandwidth, respectively.

It is assumed that for each sub-carrier, each downlink data symbol and each antenna, the same procedure is run. The following mathematical description is therefore valid for any sub-carrier. We consider the transmission of a downlink data symbol at time $t' \in [0, \tau^{DL}[$. The BS transmits the considered data symbol using the pre-computed prediction γ_k of the channel coefficient $g_k(\bar{\varepsilon})$ from the transmit antenna number k , with $\bar{\varepsilon}$ being the position vector defined in (4). The data symbol is multiplied with the maximum ratio transmission beamforming [1, 2] weight p_k . It equals the scaled complex conjugate of the predicted channel coefficient:

$$p_k = \gamma_k^* \sqrt{E}, \quad (5)$$

where $E > 0$ is a transmit power scaling factor, equal for all antennas.

We constrain the prediction γ_k to be computed based on a set of channel measurement(s) C_k . C_k is defined as the set of measurements performed for each of the $P \geq 1$ predictor antenna(s) and at $M \geq 1$ different times during the uplink frame. By definition, C_k always contain $N_{\text{meas}} = \text{card}(C_k) = P \times M \geq 1$ measurements. We define $\tau^m \in [-\tau^{UL}, 0[$ as the measurement time number m , with $m \in \Gamma = \{m \in \mathbb{N}, 0 \leq m < M\}$. With this notation, $C_k = \{\hat{g}_k(\bar{n}_l^m) | m \in \Gamma, l \in \Pi\}$, where $\hat{g}_k(\bar{n}_l^m)$ is the measurement of $g_k(\bar{n}_l^m)$ performed by the BS for the predictor antenna number l at the time τ^m .

We define the prediction horizon δ^m associated with the measurement performed at time τ^m as the delay between

- the time t' when the prediction γ_k is used for the transmission of the considered data symbol and
- the time τ^m when the channel measurement is performed before being used for the prediction γ_k .

In current standards, the subcarrier spacing is large enough so that inter carrier interference can be neglected even for high speed.

We constrain the prediction horizon δ^m to satisfy:

$$\delta^m = t' - \tau^m \geq t_0. \quad (6)$$

Finally, we here assume that measurements are perfect and noiseless:

$$\hat{g}_k(\bar{n}_l^m) = g_k(\bar{n}_l^m). \quad (7)$$

Noise-free measurements are of course an idealization. In practice, measurements are performed based on uplink pilots. These pilots are received with a finite signal to noise ratio (that we denote $\text{SNR}_{\text{pilots}}$). Channel estimates thus have errors with a normalized mean square error (NMSE) equal to $\text{NMSE}(\text{dB}) = -\text{SNR}_{\text{pilots}}(\text{dB}) - G(\text{dB})$, where the “estimator gain” G represents the noise-reduction effectiveness of a channel estimator. Kalman or Wiener filter estimators that use interpolation of several time-frequency correlated measurements can provide gains of $G = 10 - 12$ dB [13].

D. Signal-to-Noise Ratio and Energy Saving Metrics

To save energy, the BS computes the required transmit power scaling factor E that is exactly necessary to attain a target signal-to-noise ratio x_T . Since $x_T N_0$ is the total received power per unit bandwidth,

$$x_T = \frac{\left| \sum_{k \in A} \gamma_k p_k \right|^2}{N_0} = \frac{E \left| \sum_{k \in A} \gamma_k \right|^2}{N_0}, \quad (8)$$

where N_0 is the noise power per unit bandwidth at the receiver and where (5) was used in the last equality. The target transmit power scaling factor E is obtained from (8) as

$$E = x_T N_0 \left| \sum_{k \in A} \gamma_k \right|^2. \quad (9)$$

In current standards [22], the subcarrier spacing is large enough so that inter carrier interference can be neglected even for high speed. Therefore, the approximated achieved signal-to-noise ratio metric x is:

$$x = \frac{\left| \sum_{k \in A} g_k(\bar{\varepsilon}) p_k \right|^2}{N_0} = \frac{E \left| \sum_{k \in A} g_k(\bar{\varepsilon}) \gamma_k^* \right|^2}{N_0}. \quad (10)$$

By inserting (9) into (10), we obtain:

$$x = x_T \left| \sum_{k \in A} g_k(\bar{\varepsilon}) \gamma_k^* \right|^2 \left| \sum_{k \in A} \gamma_k \right|^2. \quad (11)$$

We define the energy saving metric e_s as the energy required by a SISO system divided by the energy required by the studied MISO system, for the same target signal-to-noise ratio x_T . This metric is a multiplicative factor. It measures how much less energy is consumed at the BS thanks to the use of a MISO system with a set A of base station antennas instead of a SISO system that uses only antenna $k = 0$. For instance, if $e_s = 2$, this then means that the BS uses twice less energy in MISO than in SISO. The required transmit power per unit bandwidth for a SISO system with one transmit antenna is, by (5) and (9), $|p_0|^2 = |\gamma_0|^2 E = |\gamma_0|^2 x_T N_0 |\gamma_0|^{-4} = x_T N_0 |\gamma_0|^{-2}$. For a MISO system with a set A of base station antennas, the required transmit power per unit bandwidth is $\sum_{k \in A} |p_k|^2 = \left(\sum_{k \in A} |\gamma_k|^2 \right) E = \left(\sum_{k \in A} |\gamma_k|^2 \right) x_T N_0 \left| \sum_{k \in A} |\gamma_k|^2 \right|^{-2} = x_T N_0 \left| \sum_{k \in A} |\gamma_k|^2 \right|^{-1}$. The attained energy saving for a MISO system therefore equals:

$$e_s = \frac{|p_0|^2}{\sum_{k \in A} |p_k|^2} = \sum_{k \in A} \left| \frac{\gamma_k}{\gamma_0} \right|^2. \quad (12)$$

E. Beamforming Mispointing Effect

The signal-to-noise ratio metric x and the energy saving metric e_s depend only on the channel estimate γ_k and the actual channel $g_k(\vec{e})$. If the prediction is accurate (i.e. if the channel estimate γ_k equals the actual channel $g_k(\vec{e})$), then (11) reduces to $x = x_T$, i.e. the signal-to-noise ratio target is met. Otherwise, beamforming mispointing occurs and the

signal-to-noise ratio x is expected to be different from, and in general smaller than, the target value x_T .

III. Systems Specific Models

A. Reference Systems (RS)

For RS, all antennas at the BS side are used. At the vehicle side, a single antenna is used both for prediction and for data reception. The UL/DL frames are set equal to a fixed value denoted t_0 . A single measurement from the predictor antenna is used for prediction. The prediction horizon δ^0 between the channel estimation and the data transmission is equal to the frame duration.

Using the previously defined notations, in the RS case the number of active antennas K_a equals K , the set of active antennas A becomes A_0 , the number of antennas on the vehicle L equals 1 , the number of predictor antennas P equals 1 and the index l_a of the receive antenna equals 0 . Furthermore, the uplink/downlink frames durations are $\tau^{\text{DL}} = \tau^{\text{UL}} = t_0$, the number of measurement times M equals 1 , the prediction horizon δ^0 between the channel estimation and the data transmission is $\delta^0 = t_0$.

With these assumptions, using (5) and (7), we get a simple extrapolation in time of the present channel estimate as channel predictor:

$$\gamma_k = g_k(\vec{\alpha}). \quad (13)$$

The signal-to-noise ratio metric x and the energy saving metric e_s are then derived using (1)–(6) and (10)–(12):

$$x = \frac{\left| \sum_{k \in A_0} g_k(\vec{\alpha} + t_0 \vec{v}) g_k^*(\vec{\alpha}) \right|^2}{\left| \sum_{k \in A_0} |g_k(\vec{\alpha})|^2 \right|^2} x_T, \quad (14)$$

$$e_s = \sum_{k \in A_0} \left| \frac{g_k(\vec{\alpha})}{g_0(\vec{\alpha})} \right|^2. \quad (15)$$

One can note that the signal-to-noise ratio metric x is speed-dependent whereas the energy saving metric e_s remains constant. At low speed, the signal-to-noise ratio target is met whereas mispointing occurs at high speed, thus we expect the signal-to-noise ratio to be below the target value x_T .

Fig. 4a illustrates the RS operation and Fig. 5a illustrates the resulting beamforming mispointing effect.

B. Separate Receive and Training Antennas (SRTA)

This section briefly recalls the SRTA scheme introduced in [8]. As for RS, all transmit antennas are used, and the uplink/downlink frames are equal. Prediction relies on a single measurement from a single predictor antenna, with a prediction horizon equal to the frame duration. The BS and the vehicle are assumed to have a reasonably good estimate of the speed using e.g. the Global Positioning System (GPS).

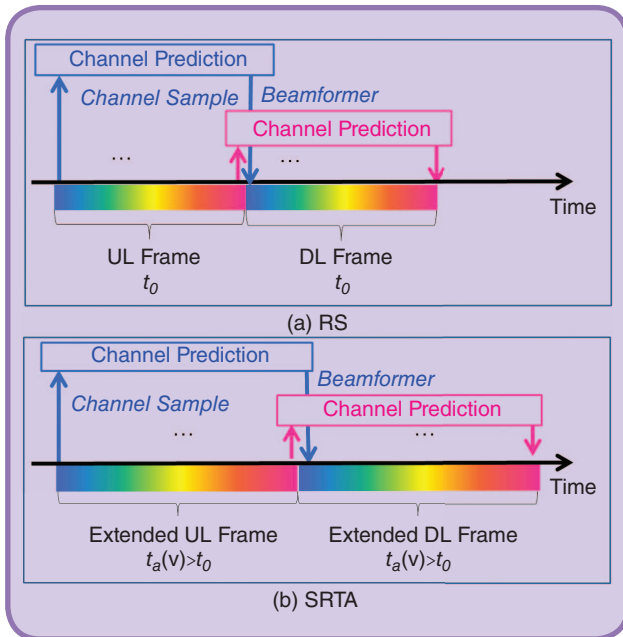


FIG 4 Frame structures for RS and SRTA schemes. Distinct beamformers are computed for distinct times during the downlink frame. Each beamformer is based on a distinct channel measurement performed during the uplink frame. All channel measurements go through the same procedure and undergo the same processing delay before being converted into beamformers.

As illustrated in Fig. 4b and Fig. 5b, SRTA avoids mispointing by selecting, according to speed, an extended frame and a suitable receive antenna among several candidate antennas located behind the predictor antenna. The receive antenna and the frame length are selected to ensure that the receive antenna is at the focusing point previously occupied by the predictor antenna, one frame duration earlier.

As for RS, the number of active antennas K_a equals K , the set of active antennas A is A_0 and the number of predictor antennas P equals l . The predictor antenna is the front antenna (with index $l = 0$) and the number of measurement times M equals 1.

Contrary to RS, the number of antennas on the vehicle L is strictly higher than 1, the frame duration $\tau^{DL} = \tau^{UL}$ and the corresponding prediction horizon δ^0 equal a speed-dependent function $t_a(v)$ which is always strictly higher than t_0 . The index of the receive antenna l_a equals a speed-dependent function $r_a(v)$.

The vehicle signals to the BS the antenna index $r_a(v)$ and the extended frame duration $t_a(v)$, where $t_a(v)$ also defines the new prediction horizon. $r_a(v)$ and $t_a(v)$ are selected by the vehicle to ensure that $\bar{\epsilon} \approx \bar{\alpha}$.

In current standards [22], frames are adaptive by steps of constant size d (such as sub-frames or slots). Reference [8] suggests to choose $r_a(v)$, $t_a(v)$ and $\bar{\epsilon}$ as functions of d , as follows.

The method for the selection of the receive antenna $r_a(v)$ is rather simple and intuitive. One can first observe that when the predictor antenna sends pilots, it is somewhat indicating to the BS the target beamforming position. One can also easily show that the time needed for the antenna number l to replace the predictor antenna, and therefore occupy the target beamforming position, is given by the duration $l\Delta v^{-1}$. Therefore, if one selects $l\Delta v^{-1}$ as the frame duration, it ensures that the antenna l is always at the target beamforming position. This is valid for any antenna l . However, the frame duration $l\Delta v^{-1}$ should be the shortest possible, to ensure that even slow moving scatterers are nearly static during the duration of the frame. Also, the frame can only be *extended* compared to t_0 .

With all these observations and requirements taken into account, it then becomes obvious that one should select the receive antenna $r_a(v)$ as the antenna l that has the smallest $l\Delta v^{-1}$ value, among all antennas having a $l\Delta v^{-1}$ value higher than t_0 . This would correspond to choosing $r_a(v)$ equal to $\min\{l \in \Lambda | l\Delta v^{-1} > t_0\}$.

However, in current standards [22], frames are adaptive by steps of constant size d (such as sub-frames or slots). Therefore, in practice, the frame duration must be set to $\lceil l\Delta (dv)^{-1} \rceil d$ instead of $l\Delta v^{-1}$. Hence, the expressions of the selected receive antenna $r_a(v)$ and the corresponding frame duration $t_a(v)$ depend on the granularity d :

$$r_a(v) = \min\{l \in \Lambda | \lceil l\Delta (dv)^{-1} \rceil d > t_0\}. \quad (16)$$

$$t_a(v) = \lceil r_a(v)\Delta (dv)^{-1} \rceil d. \quad (17)$$

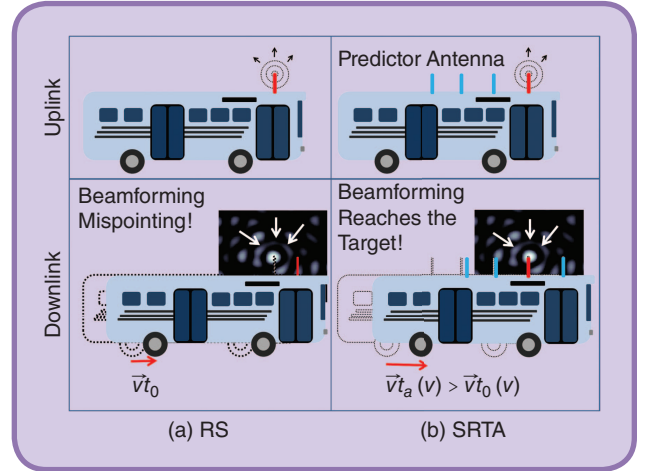


FIG 5 RS and SRTA systems. (a) In the RS system, during the delay between the channel measurement and the data transmission, the vehicle moves by a displacement $v t_0$. This causes beamforming mispointing to occur. (b) In the SRTA system, during the delay between the channel measurement and the data transmission the vehicle moves by a displacement which is compensated by the use of a predictor antenna (distinct from the receive antenna). In this case, mispointing is avoided.

The receive antenna with index $r_a(v)$ will then approximately reach the target beamforming position after the duration $t_a(v)$ of the extended frame.

Due to the granularity d , there will still remain some residual mispointing which can also be derived very intuitively. When the predictor antenna sends pilots, the position of the receive antenna relatively to the predictor antenna position is given by $-r_a(v)\Delta$. After $t_a(v)$ seconds, the receive antenna has moved by $t_a(v)v = \lceil r_a(v)\Delta (dv)^{-1} \rceil dv$ to get closer to the target beamforming position. The residual distance between the receive antenna and the target beamforming position is thus:

$$\rho(v) = \lceil r_a(v)\Delta (dv)^{-1} \rceil dv - r_a(v)\Delta. \quad (18)$$

As a consequence, the receive antenna position $\bar{\epsilon}$ can be expressed as a function of the target focusing position $\bar{\alpha}$ as follows:

$$\bar{\epsilon} = \bar{\alpha} + \rho(v)v^{-1}\bar{v}. \quad (19)$$

The relation (17) above ensures that (15) can be attained for speeds up to v_{\max} , given by $v_{\max} = (L-1)\Delta |t_0|^{-1}$. The prediction in this case is, as for RS: $\gamma_k = g_k(\bar{\alpha})$.

Finally, the signal-to-noise ratio metric x and the energy saving metric e_s are derived in [8] as follows:

$$x = \frac{\left| \sum_{k \in A_0} g_k(\bar{\alpha} + \rho(v)v^{-1}\bar{v}) g_k^*(\bar{\alpha}) \right|^2}{\left| \sum_{k \in A_0} |g_k(\bar{\alpha})|^2 \right|^2} x_T, \quad (20)$$

$$e_s = \sum_{k \in A_0} |g_k(\bar{\alpha})/g_0(\bar{\alpha})|^2. \quad (21)$$

As for RS, the signal-to-noise ratio metric x is speed dependent and the energy saving metric e_s is constant.

One can observe that some particular values of the speed do not suffer from residual beamforming mispointing, in spite of the granularity d . Let us consider a speed v for which the duration $r_a(v)\Delta v^{-1}$ is, by chance, equal to an integer number p of steps d , i.e. satisfying $r_a(v)\Delta v^{-1} = pd$. Then, equation (17) becomes $t_a(v) = [p]d = pd = r_a(v)\Delta v^{-1}$. Thus, the frame duration $t_a(v)$, luckily in this case, is exactly equal to the duration $r_a(v)\Delta v^{-1}$ required to compensate the speed. We call such a speed a “perfectly compensated” speed. All other speeds are called “non perfectly compensated” speeds.

C. SRTA with Switch Off Scheme (SOS)

SOS is used on top of SRTA to reduce the degradation in terms of signal-to-noise ratio and block error rate due to

residual beamforming mispointing for the “non perfectly compensated” speeds, as identified in section III-B. SOS detects mispointing and switches off antennas at the BS with the aim to strengthen the side beams relative to the main beam in the area of the target receiver.

As illustrated in Fig. 6, SOS (Fig. 6b) does not cancel the residual mispointing (i.e. the distance between the target beamforming position and the actual receive antenna position) of SRTA (Fig. 6a). However, it reduces the signal-to-noise ratio degradation.

SOS is a closed loop mechanism. Initially, SRTA is run with $K_a = K$ antennas. The vehicle assesses the attained signal-to-noise ratio and compares it to a threshold (in our evaluations corresponding to a 20% block error rate). If the signal-to-noise ratio is lower than the threshold, then the vehicle sends a feedback message to the BS. The BS switches off half of its antennas ($K_a = K_a/2$) and

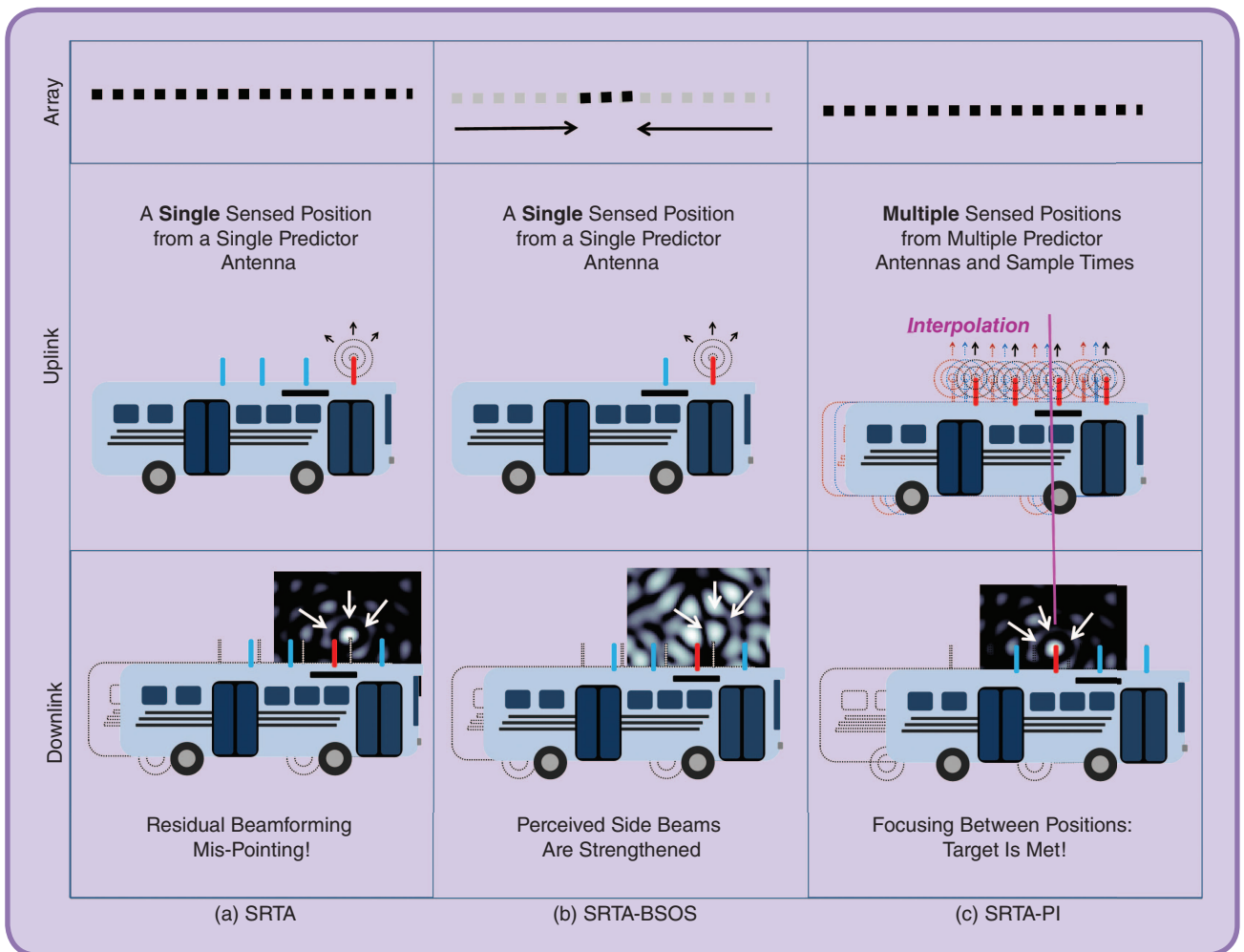


FIG 6 SRTA, SRTA-BSOS and SRTA-PI systems. (a) In the SRTA system, residual beamforming mispointing occurs for the considered speed. The target antenna receives the data with a weak power. (b) In the SRTA-BSOS system, multiple side lobes are strengthened to give more opportunities for the target antenna to receive the data with a high power. (c) In the SRTA-PI system, several channel measurements coming from several predictor antennas, and collected during the uplink frame, are interpolated to predict the channel and beamform over the exact position of the new receive antenna (the second antenna behind the front antenna).

updates A . Then, SRTA is run again with the new K_a and A parameters. K_a is successively divided by 2, until the signal-to-noise ratio threshold is exceeded. If the signal-to-noise ratio increases over a threshold, then antennas are added so the beam is narrowed. The achieved signal-to-noise ratio and energy saving are obtained by using (20), (21) with the antenna subset A used instead of the full set A_0 .

Here, the energy saving metric e_s is lower than for SRTA when A is smaller than A_0 .

Two variants of the scheme are investigated:

- SRTA Random SOS (SRTA-RSOS), which reduces the number of utilized transmit antennas without giving any preference to specific antenna positions.
- SRTA-Border SOS (SRTA-BSOS), which removes the antenna elements at the outer parts of the linear array from use in transmission, and thus reduces the array aperture.

In a pure line-of-sight propagation scenario, as illustrated in Fig. 1, the width of the transmit beam as perceived by the receiver increases when the transmit array aperture is decreased. In this case, one should use SRTA-BSOS.

In a non line-of-sight scenario, as illustrated in Fig. 2, the BS aperture as perceived by the receive antenna is no longer defined by its array size. Indeed, due to the scattering, the receive antenna sees rays arriving from many directions. In this case, there is no reason to switch off border antennas more than any other, and SRTA-RSOS might give similar or even better performance.

D. SRTA with Polynomial Interpolation (SRTA-PI)

As RS and SRTA, SRTA-PI uses $K_a = K$ transmit antennas at the BSs.

As illustrated by Fig. 6c, SRTA-PI is based on SRTA, and mitigates mispointing by focusing “between” several “sensed” positions of the predictor antennas instead of focusing “over” a single position. As illustrated in Fig. 6c and Fig. 7, multiple measurements are collected by one or multiple predictor antennas at multiple specific measurement times to obtain a dense pattern of measurements in space. Then, polynomial interpolation is applied to these measurements to predict the channel at the future position of the receive antenna. Contrary to all the previous discussed schemes, the number of measurement times M can be higher than 1. The number of predictor antennas P can also be higher than 1.

The Base Station stores a set C_k of channel measurements collected during the UL frame. A measurement $\hat{g}_k(\bar{n}_l^m)$ is collected for each predictor antenna l and at different measurement times during uplink frames. Let τ^m be the measurement time number m , with $0 \leq m < M$.

The polynomial interpolation is then performed based on C_k . For each channel measurement $\hat{g}_k(\bar{n}_l^m)$ belonging to C_k , the BS stores the couple constituted by the channel measurement $\hat{g}_k(\bar{n}_l^m)$ and the corresponding “sensed” posi-

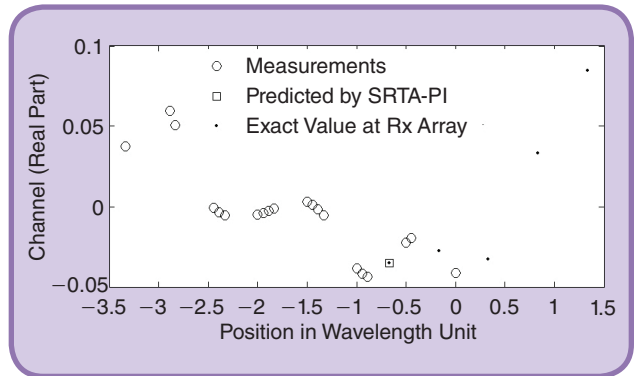


FIG 7 SRTA-PI, one channel realization at 240km/h. The real part of the channel measurements, cumulated over predictor antennas and measurement times, are plotted. Each measurement is plotted as a function of the corresponding sensed position in space. The exact values of the channel coefficients of five antennas of the vehicles at the data transmission time are also plotted. One can observe that the channel predicted for the 5th antenna obtained by interpolation of the measurements, perfectly matches the exact value.

tion \bar{n}_l^m (where $n^m \in \mathbb{R}$ is the scalar coordinate corresponding to \bar{n}_l^m , along the vehicle short term linear trajectory). Finally, the BS performs polynomial interpolation over the stored couples, with the position \bar{e} and channel γ_k as the input and output of the interpolation operation, respectively.

For a given desired prediction horizon $t_a(v)$, the receiver antenna is selected so that its position \bar{e} will be between at least two stored “sensed” positions. This enables the system to avoid extrapolation, which is less reliable than interpolation.

When polynomial interpolation is used, the frame duration need not be modified. This is an advantage of this scheme, since it reduces the system-level complexity of its use.

For ease of comparison, we will in the evaluation in section V below use the same frame length as in the other SRTA schemes, with the downlink frame duration extended compared to the RS frame: $\tau^{\text{DL}} = t_a(v) > t_0$. The extended frame duration $t_a(v)$ and the index $r_a(v)$ are then computed using (16) and (17). The index l_a of the receive antenna is selected as

$$l_a = r_a(v) + 1. \quad (22)$$

This ensures that interpolation can always be used.

Let N_{meas} be the number of measurements involved in the prediction of one channel coefficient. Polynomial interpolation is performed for the real and imaginary parts of the channel separately, with order $N_{\text{meas}} - 1$. This number of measurements N_{meas} is a critical parameter as the complexity of the polynomial interpolation increases with it. The choice of N_{meas} in the evaluation case is given in the Annex.

Due to this added polynomial interpolation operation, SRTA-PI is more complex than SRTA. At low speed, SRTA is already sufficient [8]. Therefore, to avoid unnecessary complexity, we trigger the use of polynomial interpolation for

Annex

In this annex, we detail the implementation of the SRTA-PI scheme that is used in the evaluations in section V. P is chosen equal to L to maximize the number of measurement samples. As for RS, SRTA-RSOS and SRTA-BOS, we keep the constraint of having exactly the same procedure being applied per data symbol and per sub-carrier, with the same prediction horizon. To that aim we impose the downlink frame duration to be half the uplink frame duration: $\tau^{\text{DL}} = \tau^{\text{UL}}/2$. All data symbols sent go through the same procedure, whatever the time t' at which they are sent. Though this procedure involves several distinct measurement times $\tau^m \in [-\tau^{\text{UL}}, 0]$, with $0 \leq m < M$ and several associated distinct prediction horizons $\delta^m = t' - \tau^m$, we constrain the prediction horizon δ^m to be the same for any t' .

More precisely, we constrain the prediction used for beamforming at the time t' , to be based on measurements collected during τ^{DL} seconds, at least τ^{DL} seconds before beamforming is considered, and every d seconds.

With this design, the number of measurement times becomes:

$$M = \lceil t_a(v) d^{-1} \rceil. \quad (23)$$

The expression of the measurement time number m , i.e. the parameter τ^m is then simply given by: $\tau^m = t' - t_a(v) - dm$. As a consequence, the prediction horizon δ^m equals:

$$\delta^m = t' - \tau^m = t_a(v) + dm. \quad (24)$$

By combining (23) and (24) one can verify that $t_a(v) < \delta^m \leq 2t_a(v)$. In other words, SRTA-PI does not require a shorter prediction horizon δ^m compared to the other schemes. Finally, one can note that (24) is feasible for all data symbols, i.e. for all $t' \in [0, \tau^{\text{DL}}]$, if τ^{UL} satisfies :

$$\tau^{\text{UL}} = 2\tau^{\text{DL}} = 2t_a(v). \quad (25)$$

In other words, the uplink frame needs to be twice larger than the downlink frame to ensure an identical processing and performance for all symbols of the downlink frame. The relation (22) guarantees that the position \vec{e} is between at least two stored "sensed" positions. This enables the system to avoid extrapolation, which is less reliable than interpolation. The number N_{meas} of measurements involved in the prediction of one channel coefficient is given by:

$$N_{\text{meas}} = \lceil t_a(v) d^{-1} \rceil \geq L. \quad (26)$$

speeds larger than a predefined threshold v_{PI} . For speeds lower than v_{PI} , SRTA will be used instead. The signal-to-noise ratio metric x and the energy saving metric e_s are derived using equations (11), (12), and using the prediction γ_k obtained after polynomial interpolation.

IV. Initial Comparison of the Studied Schemes

Table 1 gives an overview of the values of the parameters and an initial qualitative comparison, based on the math-

Table 1. Parameters and expected ordering.

Parameter	RS	SRTA	SRTA BSOS/RSOS	SRTA-PI
τ^{DL}	t_0		$t_a(v) > t_0$	
δ^m	t_0		$\geq t_a(v)$	
K_a	K		$\leq K$	K
L	1		> 1	
t_a	0		$t_a(v)$	$t_a(v) + 1$
P			1	$L \geq P \geq 1$
M			1	≥ 1
N_{meas}			1	≥ 2
Best x	4	3	2	1
Best e_s	1	1	2	1
Most simple	1	2	3	4

ematical expressions given in section III, in particular (11), (12), (14), (15), (20), and (21).

Regarding energy efficiency, the two SOS schemes may use a lower number K_a of active antennas, and are then expected to save less energy than RS and SRTA schemes.

Regarding the complexity, SRTA is more complex than RS as it implies the dynamic adaptation of the frame duration and the indexes of the predictor and the receive antenna. The SRTA-BSOS and SRTA-RSOS schemes are slightly more complex as they adapt the transmit array size to the speed. SRTA-PI which performs polynomial interpolation of $N_{\text{meas}} > 1$ measurements requires the highest computational complexity. However, it does not require a modification of the TDD frame duration. This makes it easier to integrate in a communication system, as compared to the other SRTA transmission schemes.

Regarding the robustness to speed of the achieved signal-to-noise ratio and the block error rate, RS should be the worst scheme as it will always suffer from beamforming mispointing. SRTA cancels mispointing for "perfectly compensated speeds" only, and should therefore be the 2nd best scheme. SOS schemes enhance SRTA for "non perfectly compensated" speeds, and should be the 3rd best. Finally, SRTA-PI completely cancels mispointing for all speeds and should hence be the best of all schemes.

V. Performance Comparison

In this section we compare the performance of the RS, SRTA-BSOS, SRTA-RSOS and SRTA-PI schemes, using simulations. We compare them in terms of robustness as measured by the attained block error rate (BLER) and in terms

of energy saving, using the energy saving metric e_s defined in section II-D.

A. Simulation Assumptions and Methodology

The following simulation assumptions are used. The required minimal prediction horizon is $t_0 = 2$ ms [22]; the carrier frequency f_0 is 2 GHz; the wavelength is $\lambda = c/f_0$; where $c = 3 \cdot 10^8$ m/s is the speed of light. The BS has a linear array with $K = 64$ antennas separated by $\lambda/2$. In SRTA and SRTA-BSOS/RSOS the vehicle has $L = 4$ antennas separated by Δ , with $\Delta = \lambda/2$. For SRTA-PI, $L = 5$. The time step for frame extension is $d = 1$ ms, which is feasible in current standards [22]. It is also used for SRTA-PI measurements selection. The vehicle speed v ranges from 0 to 300 km/h. The target SNR is $x_r = 15.5$ dB, which corresponds to a target BLER of 0.01 for 64QAM with code rate 3/4. $v_{PI} = 50$ km/h is chosen to trigger PI, for SRTA-PI.

In all studied systems, the same procedure, with the same prediction horizon(s), is applied to perform the transmission of any downlink data symbol over any sub-carrier. We therefore model and assess the performance of the studied systems on a single downlink data symbol and sub-carrier basis. The performance is assessed for each symbol, and the final result is averaged over 1000 symbols.

For each simulated data symbol, channel coefficients for the uplink channel measurement and for the downlink data transmission phases are generated. These channel coefficients are correlated in the spatial and temporal domains. The angle giving the direction of the BS antenna array and the angle of the vector \vec{v} are generated randomly and are uniformly distributed between 0 and 2π . The position vector $\vec{\alpha}$ is also generated randomly. All other positions are deduced from $\vec{\alpha}$ and \vec{v} . Channel coefficients are then generated using a spatially correlated Ricean channel model with a line-of-sight to total power ratio factor R which is either equal to 0 or 0.8. $R = 0$ corresponds to non line-of-sight. For $R = 0.8$, the channel is dominated by the line-of-sight component. We apply the method used to generate space-time correlated propagation channel coefficients for a scattering environment in [23] to our particular scenario. The propagation channel is modeled as a sum of the contributions of several planar waves. Each planar wave (or ray) is characterized by a random complex amplitude, a random angle of departure and a random angle of arrival (with angles uniformly distributed between 0 and 2π).

For each simulated data symbol, the following metrics are computed for various values of the speed v : the downlink frame duration τ^{DL} , the selected receive antenna index l_a , the number of active antennas K_a the signal-to-noise ratio metric x and the energy saving metric e_s . As the simulations are performed on a data symbol basis, only the data symbol error rate can be derived in a straight forward manner from the signal-to-noise ratio. However, in this paper,

we will assume that all the data symbols within a data block are likely to be received with the same signal-to-noise ratio even for very high speed. Although the channel certainly differs from one data symbol to the other at high speed, the “width” of the beam and the corresponding mispointing is similar from one data symbol to the other. It mainly depends on the number of transmit antennas and the Ricean channel parameter R . In this paper, we will therefore deduce the block error rate (or the block error probability) from the signal-to-noise ratio x using results stored in Table 2 based on link level simulations with constant channels and additive white Gaussian noise.

All the previously listed metrics are stored for each simulated data symbol and each speed v , then averaged over data symbols, and plotted as a function of speed v .

B. Robustness and Energy Efficiency

In this sub-section, a non line-of-sight propagation channel model is used. This will therefore illustrate the scenario of Fig. 2.

Fig. 8 illustrates the index l_a of the selected receive antenna as a function of v . RS only uses a single antenna, therefore $l_a = 0$. For all SRTA schemes, the receive antenna is selected farther behind the predictor antenna to compensate higher speeds. As discussed in section III-C, the SRTA and SRTA-RSOS/BSOS schemes use the same antenna selection. As explained in section III-D, SRTA-PI uses a farther antenna than SRTA to avoid extrapolation. Fig. 9 illustrates the downlink frame duration $t_a(v)$ as a function of the speed v . As explained in section IV, all SRTA schemes use

Table 2. BLER for 64 QAM, rate 3/4, turbo code, with block length of 6000 bits.

SNR	14.5	15.0	15.5	15.7	16.0
BLER	1.0	0.8205	0.0125	0.0028	0.000001

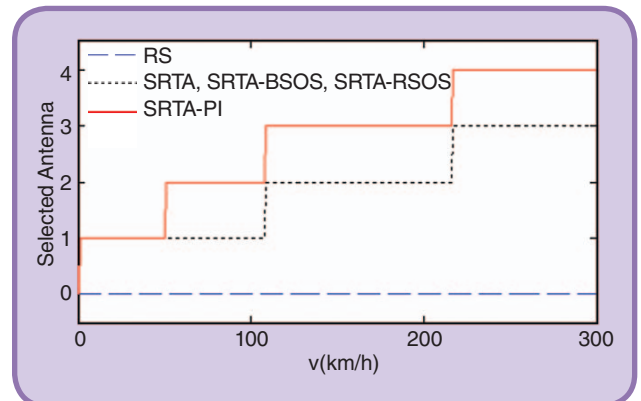


FIG 8 Selected antennas for downlink reception.

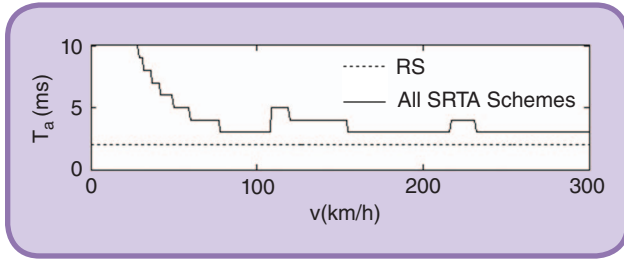


FIG 9 Extended frame versus vehicle speed.

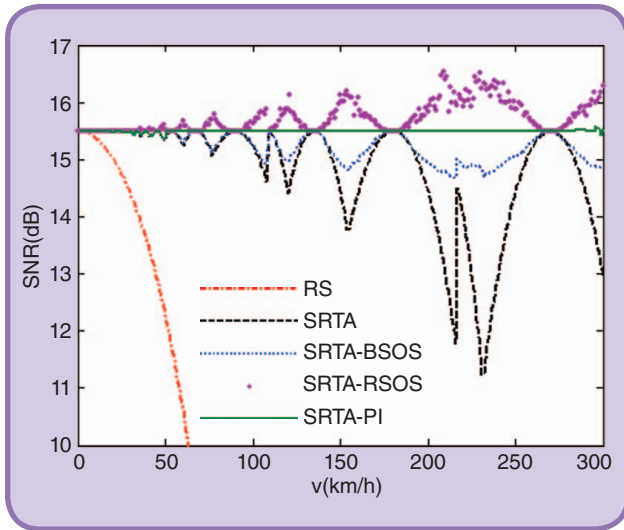


FIG 10 SNR versus speed.

the same $t_a(v)$ value, which decreases with speed but is always strictly higher than t_0 , thus higher than for RS.

Fig. 10 and 11 illustrate the signal-to-noise ratio and the block error rate as a function of the speed v , respectively. With RS, the performance degrades strongly for speeds larger than 50 km/h, reaching a block error rate of 1. This is due to the mispointing effect described in the introduction and in section II-E. Note that in Table 2 the block error rate is a sensitive function of the attained signal-to-noise ratio. In Fig. 10 and 11, one can observe some particular speed values, for which SRTA achieves the target signal-to-noise ratio and the target block error rate. As explained in section III, these are the “perfectly compensated speeds”. SRTA is efficient for “perfectly compensated” speeds but not “non perfectly compensated” speeds. The discontinuities observed on Fig. 9–13 at speeds around 110 km/h and 225 km/h are due to the changes of selected antenna (see Fig. 8). SRTA-BSOS/RSOS better handles “non perfectly compensated” speeds by reducing degradation in terms of signal-to-noise ratio and block error rate. RSOS outperforms BSOS as an irregular pattern of switched-off transmit antennas creates a tapering [24] effect.

Fig. 12 and 13 illustrate the number of active transmit antennas K_a and the corresponding energy saving e_s as a

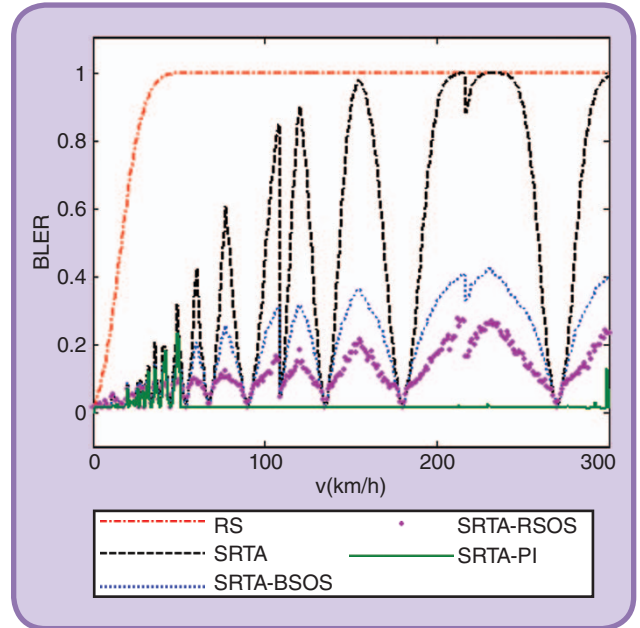


FIG 11 BLER versus speed.

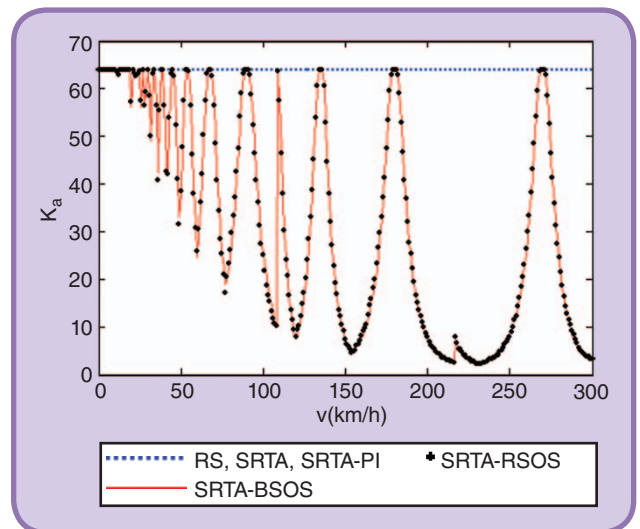


FIG 12 Number of active antennas versus speed.

function of the speed v , respectively. RS and SRTA use all antennas and achieve the maximum energy saving. For “perfectly compensated” speeds, SRTA-BSOS/RSOS behave like SRTA, whereas for “non perfectly compensated” speeds, $K_a < K$ antennas are used and less energy is saved. In other words, SOS schemes sacrifice energy saving to get better robustness of the block error rate against speed.

As illustrated by Fig. 10–13, SRTA-PI perfectly compensates all speeds larger than $v_{PI} = 50$ km/h, and still with maximum energy saving. For lower speeds, the polynomial interpolation is not triggered (as specified in III-D), as SRTA is sufficient. SRTA-PI therefore outperforms SRTA-RSOS with respect to energy saving and robustness.

These simulation results confirm the ordering identified in section IV.

C. Impact of the Channel (Partial Line-of-Sight Versus Non Line-of-Sight Propagation)

In this section simulations are run with a Rice fading model with Rice factor $R = 0.8$, i.e. with a dominating line-of-sight component. Although the received power is here dominated by line-of-sight components, the short-term fading within the beam is still very significant. This results in a high BLER for the RS scheme at velocities above 20 km/h. A comparison between Fig. 14 to Fig. 11 shows that the RS and SRTA schemes undergo a somewhat stronger mispointing effect in complete non line-of-sight (Fig. 11) than in partial line-of-sight conditions (Fig. 14). Not included here, the same observations are obtained when making the comparison between partial line-of-sight and non line-of-sight w.r.t. the energy saving and the signal-to-noise ratio instead of the block error rate. This is not surprising, as it has been shown that scattering increases spatial focusing of Time Reversal beamforming [25] which is similar to maximum ratio transmission beamforming [26]. Indeed, scatterers surrounding the transmit and the receive antenna arrays virtually increase the apertures of these arrays. As a consequence, the focused beam is narrower.

VI. Conclusion

In this study we illustrated how the use of predictor antennas can render an adaptive antenna technique as efficient for vehicular communications as it is for static communications. We proposed three new schemes to provide more robust energy efficient wireless downlink data transmission towards antennas upon very fast moving vehicles. All these schemes exploit the predictor antenna concept, an elastic frame and beamforming. The two first schemes, the “Border Switch Off Scheme” and the “Random Switch Off Scheme” simply switch off transmit antennas to decrease the influence of the short-term fading when beamforming mispointing is too severe. They slightly improve robustness but reduce the energy savings. The third “Polynomial Interpolation” scheme is robust to all speeds up to 300 km/h and achieves maximum energy saving. This latter scheme relies on a Predictor Antennas Array and Polynomial Interpolation over multiple measurement samples. Ongoing studies focus on reducing its complexity, while keeping its ability to perfectly control the block error rate at any speed.

The techniques used at the vehicle side are variants of the separate receive and transmit antenna (SRTA) scheme. They require multiple antenna elements but are of low complexity since they constitute antenna switching between the antennas on the vehicle. This requires only one receive radio frequency amplification and processing chain.

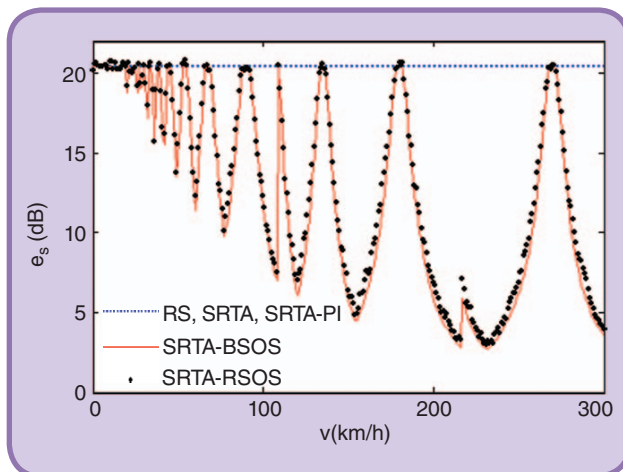


FIG 13 Energy saving versus speed.

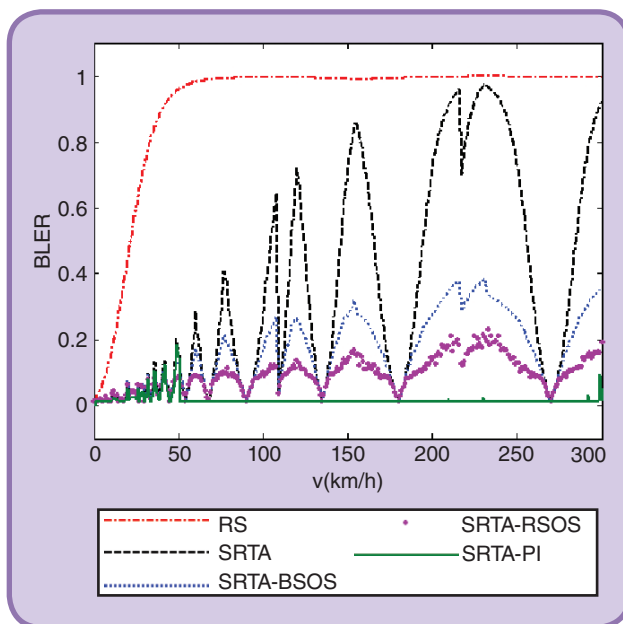


FIG 14 BLER versus speed, strong line-of-sight.

The concept of using predictor antennas is more general, and could be used in combination with more sophisticated multi-antenna receivers. Examples include maximum ratio combining or interference rejection combining at reception, iterative interference cancellation receivers or MIMO multiplexing of multiple data streams. Use of predictor antennas could also be integrated into conventional Kalman predictors, to maximize the use of all collected channel samples and antennas.

About the Authors

Dinh-Thuy Phan-Huy (dinhthuy.phanhuy@orange.com) received her Masters degree of Electrical and Computer Engineering from Supelec in 2001. She is with Orange since 2001 and is currently working as a research engineer in



Orange Labs Networks. She has led the French National research project TRIMARAN on time reversal space-time focusing technique from February 2011 to August 2014. She is also involved the FP7 METIS project targeting solutions for 2020. Her main research interests are multi-antenna techniques.



Mikael Sternad (M'88, SM'90) (mikael.sternad@signal.uu.se) is a professor of automatic control at Uppsala University and received a Ph.D. degree from Uppsala University in the same field in 1987. He is leading the Dynamic Multi-point Wireless Access framework project funded by the Swedish Research Council. He is currently also active in the EU FP7 METIS project targeting solutions for 2020. Channel prediction has been one focus area of research for 15 years. He is also involved in audio and acoustic MIMO signal processing, room compensation, and sound field control. He co-founded and was chairman (2001–2005) of Dirac Research, a company in this area.



Tommy Svensson (M'05, SM'10) (tommy.svensson@chalmers.se) is an associate professor in communication systems at Chalmers University of Technology, where he is leading the research on air interface and microwave backhaul networking technologies for future wireless systems. He received a Ph.D. in information theory from Chalmers in 2005. He is currently active in the EU FP7 METIS project targeting solutions for 2020. His main research interests are in design and analysis of physical layer algorithms, multiple access, resource allocation, cooperative systems, moving relays/cells/networks, as well as satellite systems. He is chairman of the IEEE Sweden Vehicular Technology/Communications/Information Theory chapter, and coordinator of the Communication Engineering Master's Program at Chalmers.

References

- [1] T. K. Y. Lo, "Maximum ratio transmission," *IEEE Trans. Commun.*, vol. 47, no. 10, pp. 1458–1461, 1999.
- [2] A. Paulraj, R. Nabar, and D. Gore, *Introduction to Space-Time Wireless Communications*. New York: Cambridge Univ. Press, 2008.
- [3] S. K. Mohammed, A. Chockalingam, and B. S. Rajan, "A low-complexity precoder for large multiuser MISO systems," in *Proc. IEEE Vehicular Technology Conf.*, May 2008, pp. 797–801.
- [4] H. Yang and T. L. Marzetta, "Performance of conjugate and zero-forcing beamforming in large-scale antenna systems," *IEEE J. Select. Areas Commun.*, vol. 31, no. 2, pp. 172–179, Feb. 2013.
- [5] S. Wagner, R. Couillet, M. Debbah, and D. Slock, "Large system analysis of linear precoding in correlated MISO broadcast channels under

limited feedback," *IEEE Trans. Inform. Theory*, vol. 58, no. 7, pp. 4509–4537, 2012.

- [6] A. Osseiran, V. Braun, T. Hidekazu, P. Marsch, H. Schotten, H. Tullberg, M. A. Uusitalo, and M. Schellman, "The foundation of the mobile and wireless communications system for 2020 and beyond: Challenges, enablers and technology solutions," in *Proc. IEEE Vehicular Technology Conf.*, June 2015, pp. 1–5.
- [7] K. T. Truong and R. W. Heath, "Effects of channel aging in massive MIMO systems," *J. Commun. Netw.*, vol. 15, no. 4, pp. 358–351, Aug. 2013.
- [8] D.-T. Phan-Huy and M. H elard, "Large MISO beamforming for high speed vehicles using separate receive & training antennas," in *Proc. IEEE Int. Symp. Wireless Vehicular Communication*, June 2015, pp. 1–5.
- [9] T. Ekman, G. Kubin, M. Sternad, and A. Ahl en, "Quadratic and linear filters for mobile radio prediction," in *Proc. IEEE Vehicular Technology Conf. Fall*, Amsterdam, The Netherlands, Sept. 19–22, 1999.
- [10] T. Ekman, A. Ahl en, and M. Sternad, "Unbiased power prediction on Rayleigh fading channels," in *Proc. IEEE Vehicular Technology Conf. Fall*, Vancouver, BC, Canada, Sept. 2002, pp. 280–284.
- [11] T. Ekman. (2002). Prediction of mobile radio channels: Modeling and design. Ph.D. dissertation, Signals and Syst., Uppsala Univ., Uppsala, Sweden. [Online]. Available <http://www.signal.uu.se/Publications/pdf/a025.pdf>
- [12] A. Duel-Hallen, "Fading channel prediction for mobile radio adaptive transmission systems," in *Proc. IEEE*, vol. 95, no. 12, pp. 2299–2315, Dec. 2007.
- [13] D. Aronsson. (2011, Mar.). Channel estimation and prediction for MIMO OFDM systems—Key design and performance aspects of Kalman-based algorithms. Ph.D. dissertation, Signals and Syst., Uppsala Univ., Uppsala, Sweden. [Online]. Available: <http://www.signal.uu.se/Publications/pdf/a112.pdf>
- [14] M. Sternad, M. Grieger, R. Apelfr ojd, T. Svensson, D. Aronsson, and A. B. Martinez, "Using "predictor antennas" for long-range prediction of fast fading for moving relays," in *Proc. IEEE Wireless Communications Networking Conf. Workshops*, Apr. 2012, pp. 255–257.
- [15] Y. Sui, J. Vihri al a, A. Papadogiannis, M. Sternad, W. Yang, and T. Svensson, "Moving cells: A promising solution to boost performance for vehicular users," *IEEE Commun. Mag.*, vol. 51, no. 6, pp. 62–68, June 2015.
- [16] A. B. Martinez, "Using "predictor antennas" for long-range prediction of fast fading for moving relays," M.S. thesis, Technische Univ. Dresden, Dresden, Germany, Aug. 20, 2012.
- [17] N. Jamaly, R. Apelfr ojd, A. B. Martinez, M. Grieger, T. Svensson, M. Sternad, and G. Fettweis, "Analysis and measurement of multiple antenna systems for fading channels prediction in moving relays," in *Proc. European Conf. Antennas Propagation*, Hague, The Netherlands, Apr. 2014.
- [18] M. Grieger and G. Fettweis, "Field trial results on uplink joint detection for moving relays," in *Proc. IEEE 8th Int. Conf. Wireless Mobile Computing, Networking Communication*, 2012, pp. 586–592.
- [19] I. Wiklund. (2012, Aug.). Channel prediction for moving relays. M.S. thesis, Uppsala Univ., Uppsala, Sweden. [Online]. Available: <http://uu.diva-portal.org/smash/record.jsf?pid=diva2:607338>
- [20] N. Jamaly, "Multiport antenna systems for space-time wireless communications," Ph.D. dissertation, Commun. Syst. Group Dept. Signals Syst., Chalmers Univ. Technol., Gothenburg, Sweden, 2015.
- [21] W. Zirwas, T. Giebel, H. Rohling, E. Schulz, and J. Eichinger, "CSI-estimation for cooperative antennas," in *Proc. Int. OFDM Workshop*, Hamburg, Germany, Sept. 2005.
- [22] 5GPP, "Physical channels and modulation (Release 10)," Technical Specification Group Radio Access Network; Evolved Universal Terrestrial Radio Access (E-UTRA), Tech. Rep. TS56.211, Dec. 2012.
- [23] P. Ky osti, et al., "WINNER II channel models," Tech. Rep. IST-4-027756 Winner II D1.1.2 V1.2, Sept. 30, 2007.
- [24] C. Balanis, *Antenna Theory: Analysis and Design*, 2nd ed. New York: Wiley, 1997.
- [25] A. Derode, A. Tourin, J. D. Rosny, M. Tanter, S. Yon, and M. Fink, "Taking advantage of multiple scattering to communicate with time-reversal antennas," *Phys. Rev. Lett.*, vol. 90, pp. 014301-1–014301-4, Jan. 2005.
- [26] T. Dubois, M. H elard, M. Cruss iere, and C. Germond, "Performance of time reversal precoding technique for MISO-OFDM systems," *EURASIP J. Wireless Commun. Netw.*, Nov. 2015.
- [27] D.-T. Phan-Huy, M. Sternad, and T. Svensson, "Adaptive large MISO downlink with predictor Antenna array for very fast moving vehicles," in *Proc. Int. Conf. Connected Vehicles Expo.*, Dec. 2015, pp. 351–356.